Special Issue: Positioning of Tissue Engineering in Regenerative Medicine

Original Article

Preparation of biodegradable iron oxide nanoparticles with gelatin for magnetic resonance imaging

Asahi Tomitaka[1)], Jun-ichiro Jo[2)], Ichio Aoki[2)], and Yasuhiko Tabata[1, *)]

[1)]Institute of Frontier Medical Sciences, Kyoto University, Kyoto, Japan
[2)]Molecular Imaging Center (MIC), National Institute of Radiological Sciences (NIRS), Chiba, Japan

The objective of this study is to prepare biodegradable iron oxide nanoparticles with bioabsorbable gelatin. Nano-size gelatin composites with well-dispersed structure of ultra-small iron oxide nanoparticles within a gelatin nanoparticle were prepared by a micro-emulsion method. The gelatin iron oxide nanoparticles prepared were degraded with time in 20 mM citric acid buffer solution at pH 4.5, in remarked contrast to gelatin iron oxide nanoparticles prepared by the conventional co-precipitation method. When co-cultured with human bone marrow-derived mesenchymal stem cells, the gelatin iron oxide nanoparticles were internalized into cells and degraded with time intracellularly. The biodegradable gelatin iron oxide nanoparticles showed the T2-weighted signals of magnetic resonance imaging.

Rec.12/17/2013, Acc.12/19/2013, pp45-55

* Correspondence should be addressed to:
Yasuhiko Tabata, Institute for Frontier Medical Sciences, Kyoto University, 53 Kawahara-cho Shogoin, Sakyo-ku, Kyoto 606-8507, Japan. Phone: +81(75)751-4121, Fax: +81(75)751-4646, E-mail: yasuhiko@frontier.kyoto-u.ac.jp

Key words biodegradation, cellular internalization, gelatin, iron oxide nanoparticles, MRI

Introduction

Nanoparticles have a potential for biomedical and pharmaceutical applications because of their small size, large surface-to-volume ratio, and the easiness of surface modification[1)]. Moreover, the characteristics of nanoparticles are different from those of bulk materials. Among them, iron oxide nanoparticles have been explored and applied for biomedical applications, such as magnetic resonance imaging (MRI)[2, 3)], biosensor, drug delivery system[1, 29)], gene delivery[4,5)], cell separation[6)], and hyperthermia treatment[7)]. Various iron oxide nanoparticles have been developed focusing on the control of particle monodispersity in size and magnetic properties, the surface coating of nanoparticles for the water solubilization, and the surface functionalization of nanoparticles with targeting molecules[8-14)]. Highly monodisperse iron oxide nanoparticles with the size distribution less than 3.2 % and 5 % were prepared by thermal decomposition, respectively[8,9)]. The nanoparticles are functionalized

by their coating with poly(ethylene glycol) (PEG)[10], polyethylenimine (PEI)[11], other polymers[12, 13], and fatty acids[14]. The surface functionalization of iron oxide nanoparticles improved their cellular internalization efficiency and targeting ability to a specific site in the body[15,16]. However, one of the iron oxide nanoparticles-related problems is their no-degradability. There are only a few reports to investigate the biodegradability of iron oxide nanoparticles[17-19]. No researches have been reported on the design of iron oxide nanoparticles which can be degraded *in vitro*.

Gelatin is a biodegradable polymer prepared from the denaturation of collagen and has been utilized for medical and pharmaceutical applications. Gelatin is chemically crosslinked to form hydrogels which achieve the controlled release of proteins and low-molecular-weight drugs[20-23]. In addition, gelatin nanospheres have been reported to be a good carrier of gene transfection[24, 25].

In this study, this biodegradable gelatin of carrier material was used to prepare iron oxide nanoparticles. If ultrasmall iron oxide nanoparticles are dispersed in the matrix of gelatin, the degradability of iron oxide will be improved. A micro-emulsion method was introduced to design the nano-size composite of iron oxide nanoparticles with gelatin. The *in vitro* degradability of gelatin iron oxide nanoparticles was evaluated in a citric acid buffer solution at pH 4.5 and human mesenchymal stem cells. We examined the MRI relaxivity of gelatin iron oxide nanoparticles.

Materials and Methods

1)Materials

Gelatin with an isoelectric point (pI) of 9.0 (Mw=100,000), prepared by an acidic treatment of pig skin, was kindly supplied from Nitta Gelatin Inc., Osaka, Japan. Ferrous chloride, poryoxyethylene sorbitan monooleate (Tween 80), 2,2,4-trimethylpentane (isooctane), glutaraldehyde (25 wt% in water), ammonia solution, citric acid anhydrous, 1M sodium hydroxide solution, L(+)-ascorbic acid, bathophenanthroline disulfonic acid, cell count reagent SF, 1M hydrochloric acid, and 6M hydrochloric acid were purchased from Nacalai Tesque. Inc., Kyoto, Japan. Ferric chloride, sorbitan monooleate (Span 80), and potassium hexacyanoferrate (II) were purchased from Wako Pure Chemical Industries, Ltd., Osaka, Japan. Nuclear fast red was purchased from Sigma-Aldrich Inc., St. Louis, MO, USA. They were used without further purification.

2)Preparation of iron oxide nanoparticles with gelatin by micro-emulsion method

Nano-sized composites of iron oxide nanoparticles with gelatin (gelatin iron oxide nanoparticles) were prepared by the micro-emulsion method with slight modification (Fig.1 (a)). The preparation was performed with three micro-emulsions of M(I), M(II), and M(III). For the preparation of M(I), 50 μl of 111 mg/ml Ferric chloride was added to 2 ml of 1 mg/ml gelatin solution, followed by mixing for 30 min at room temperature. Then, 50 μl of 41 mg/ml ferrous chloride was added to the solution. This resulting solution was dispersed in 40 ml of isooctane containing 480 mg of Span

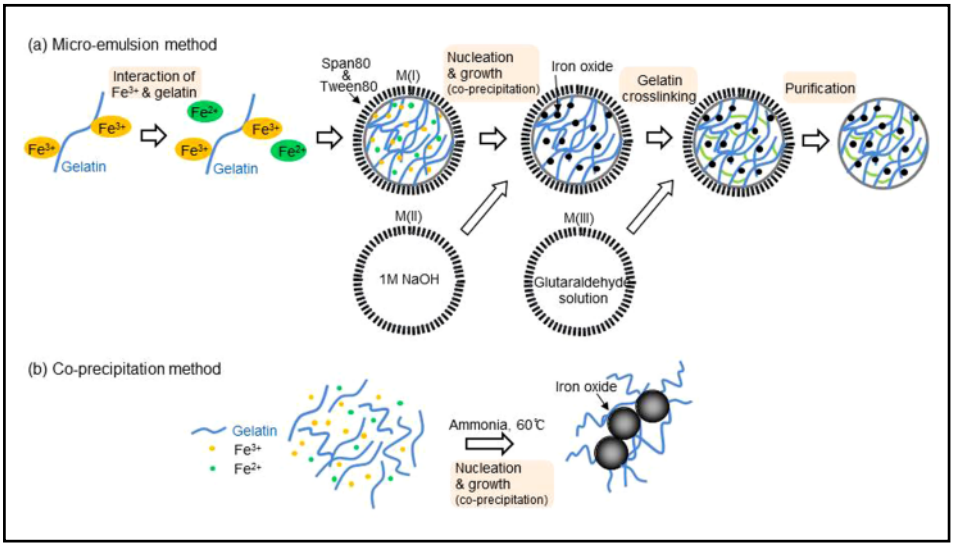

Fig.1 Schematic representation of (a) gelatin iron oxide nanoparticles prepared by the micro-emulsion method, and (b) gelatin iron oxide nanoparticles prepared by the co-precipitation method.

80 and 480 mg of Tween 80, and then sonicated for 3 min at room temperature under N_2 bubbling to obtain the micro-emulsion M(I). For the M(II), 200 μl of 1 M-sodium hydroxide solution was dispersed in 40 ml of isooctane containing 480 mg of Span 80 and 480 mg of Tween 80, and sonicated for 3 min at room temperature under N_2 bubbling. To prepare the micro-emulsion M(III), 200 μl of 0.5 wt% glutaraldehyde solution was dispersed in 40 ml of isooctane containing 480 mg of Span 80 and 480 mg of Tween 80, and sonicated for 3 min at room temperature under N_2 bubbling. The M(II) micro-emulsion was added to the M(I) and sonicated for 3 min on ice under N_2 bubbling, and then the M(III) was added to the mixed M(I) and M(II) micro-emulsion. Following sonication for 3 min on ice under N_2 bubbling, the final solution was stirred overnight at 4 ℃, washed 3 times with acetone, and freeze-dried to obtain gelatin iron oxide nanoparticles.

3)Preparation of iron oxide nanoparticles with gelatin by co-precipitation method

A control material of iron oxide nanoparticles was prepared by the conventional co-precipitation method (Fig.1 (b))[26]. Briefly, 120 μl of 100 mg/ml ferric chloride and 41 mg/ml ferrous chloride was added to 1 ml of 20 mg/ml gelatin aqueous solution. The molar ratio of ferric ions to ferrous ions was 1.8. Then, 250 μl of 28 vol% ammonia aqueous solution was added to the solution and incubated at 60℃ for 20 min. The suspension was desalted by the PD-10 column (GE Healthcare Bio-Sciences Corp., Piscataway, NJ, USA) with double-distilled water (DDW).

4)Characterization of gelatin iron oxide nanoparticles

The morphology of gelatin iron oxide nanoparticles prepared by the micro-emulsion and co-precipitation methods was observed by transmission electron microscopy (TEM, Hitachi H-7650, Hitachi, Tokyo, Japan). The freeze-dried gelatin iron oxide nanoparticles were dispersed in DDW. The dispersion was dropped onto a grid, and the grid was air-dried at room temperature for the TEM observation.

The hydrodynamic sizes and surface potentials of gelatin iron oxide nanoparticles were measured by Zetasizer Nano-ZS (Malvern instruments, Worcestershire, UK). The freeze-dried gelatin iron oxide nanoparticles of sample were dispersed in 10 mM phosphate buffered-saline solution (PBS, pH7.4).

The magnetization curve of freeze-dried nanoparticles was measured using a superconducting quantum interference device (SQUID, Quantum Design, San Diego, CA, USA) at room temperature at a maximum field of 7 T.

5)Magnetic resonance imaging (MRI) of gelatin iron oxide nanoparticles

The MRI property of gelatin iron oxide nanoparticles was evaluated in a 7.0 T, 20 cm bore horizontal magnet interfaced to a BioSpec 70/20 AVANCE-III system (Bruker Biospin, Ettlingen, Germany). A 60 mm diameter birdcage coil (transmission and reception, Bruker Biospin, Ettlingen, Germany) was used for measurement. An aqueous solution of nanoparticles (100 μl) was placed into a polymerization chain reaction (PCR) tube (200 μl) cluster plate (Simport Plastics Ltd., Beloeil, Canada). Sample temperature was maintained at room temperature. The longitudinal relaxation time (T_1)-weighted images were obtained using a conventional spin echo (SE) sequence with the following parameters: pulse repetition time (TR) = 400 ms; echo time (TE) = 9.57 ms; matrix size = 256 x 256; field of view (FOV) = 38.4 × 38.4 mm; slice thickness (ST) = 2.0 mm; and number of acquisitions (NA) = 4. The total acquisition time for three slices was 6.8 min. Two dimensional image was carried out using a fast SE acquisition inversion recovery pulse for T_1 map calculation with the following parameters: TR = 10,000 ms, TE = 20 ms, inversion time (TI) = 52.0, 100, 200, 400, 800, 1,600, 3,200, and 6,400 ms, NA = 1, and rapid acquisition with relaxation enhancement (RARE) factor =4. Total acquisition time was 42.7 min. The longitudinal relaxivity (R_1) was calculated by the following formula; $R1 = (1/T_1 - 1/T_0) / C$, where T_0 is the longitudinal time of double-distilled water (DDW) and C is the corresponding Fe^{3+} concentration. On the other hand, the transverse relaxation time (T_2)-weighted images were also obtained using a conventional SE sequence with the following parameters: TR = 3000 ms; TE = 60 ms; and NA = 1. Two dimensional single-slice multi-echo imaging was performed to generate T_2 maps with the following parameters: TR = 3,000 ms, TE = 10, 20, 30, 40, 50, 60, 70, 80, 90, and 100 ms; and NA = 1. The total acquisition time for multi-echo imaging was 12.8 min. The transverse relaxivity (R_2) was calculated by the following formula; $R_2 = (1/T_2 - 1/T_0) / C$.

6) *In vitro* degradation test of gelatin iron oxide nanoparticles

Citric acid buffer (20 mM) was prepared by dissolving citric acid in PBS. The pH of the buffer was adjusted at 4.5 by adding 1 M sodium hydroxide solution. The gelatin iron oxide nanoparticles prepared by the micro-emulsion and co-precipitation methods were placed in 20 mM citric acid buffer at pH 4.5 to give the concentration of 25 μgFe/ml, followed by incubation at 37℃ for 7 days. The concentration of free Fe(III) was measured 0.5, 1, 2, 4, 8, 16, and 24 hr, or 2, 3, 5, 7 days after incubation for gelatin iron oxide nanoparticles. For the Fe(III) measurement, the nanoparticles solution was centrifuged at 20,000 g for 5 min at room temperature, and the supernatant was collected. The supernatant (100 μl) was mixed with 2 μl of 100 mM ascorbic acid, then 4 μl of 4.95 mM bathophenanthroline disulfonic acid was added to the mixed solution. After 15 min, the absorbance was measured at the wavelength of 535 nm on a VERSAmax microplate reader (Molecular Devices, Sunnyvale, CA, USA).

7) Cell culture

Human bone marrow-derived mensenchymal stem cells were kindly provided from Prof. Junya Toguchida, Institute for Frontier Medical Sciences, Kyoto University. The cells were cultured in low-glucose Dulbecco's modified Eagle medium (DMEM, GIBCO Lifetechnologies Co., Carlsbad, CA, USA) supplemented with 10 vol% bovine fetal calf serum (FCS, Hyclone laboratories, Inc., Utah, UT, USA) and 1 wt% mixed penicillin and streptomycin solution (Sigma-Aldrich Inc., St. Louis, MO, USA) at 37℃ in humidified atmosphere of 5% CO_2 / 95% air. The cells proliferated were detached with 0.25 wt% trypsin-containing 0.8 mM ethylenediaminetetracetic acid solution in PBS, and re-suspended in the medium for following experiments.

8) Cellular internalization of gelatin iron oxide nanoparticles and intracellular degradation

The cells were seeded on each well of 12 multi-well cluster plate (Corning Inc., NY, USA) at a density of 5×10^4 cells/well and cultured in 1 ml of medium for 24 hr. The medium was exchanged by 1 ml of fresh medium containing 200 μg/ml of gelatin iron oxide nanoparticles. After 24 hr of incubation, the cells were washed with PBS three times, detached with 0.25 wt% trypsin-containing 0.8 mM ethylenediaminetetracetic acid solution in PBS, and then re-seeded on each well of 12 multi-well cluster plate. Prussian blue staining for the iron amount determination was performed 0, 1, 2, 4, and 6 days after incubation.

The Prussian blue staining was performed to investigate the localization of gelatin iron oxide nanoparticles in mesenchymal stem cells. Briefly, after incubation with nanoparticles, 4 wt% paraformaldehyde was added, followed by incubation at 4℃ for 5 min for cell fixation. Then, 1 ml of solution containing 5 wt% potassium ferrocyanide and 10 vol% hydrochloric acid was added to each well, and cells were incubated at room temperature for 20 min. After washing with DDW 3 times, the cells were counter-stained with nuclear fast red solution for 5 min, followed by washing with DDW 3 times. The cells picture was taken by an Olympus AX80 microscope (Olympus, Tokyo, Japan) through an AxioCam HRc digital camera (Carl Zeiss, Oberkochen, Germany).

To measure the amount of gelatin iron oxide nanoparticles internalized into cells, the cells were lysed with concentrated hydrochloric acid. After an appropriate dilution of lysate with DDW, the amount of iron in the diluent was measured by an atomic absorption spectrophotometer (AA-6800, Shimadzu Co., Kyoto, Japan).

9) Magnetic separation of mesenchymal stem cells

The cells were seeded on each well of 12 multi-well cluster plate (Corning Inc., NY, USA) at a density of 5×10^4 cells/well and cultured in 1 ml of medium for 24 hr. The medium was exchanged by 1 ml of fresh medium containing 200 μg/ml of gelatin iron oxide nanoparticles. After 24 hr of incubation, the cells were washed with PBS 3 times, detached with 0.25 wt% trypsin-containing 0.8 mM ethylenediaminetetracetic acid solution in PBS, and transferred to a 1.5-ml Eppendorf tube to prepare a cell suspension. The cell suspension was incubated for 1 hr with a NdFeB magnet (Remanence B_r, 1.17.1.32 T) exposed to the tube. Then, medium was collected to count the number of cells unattached to the magnet. Then, fresh medium was added to the tube while the number of cells attached was counted.

10) Cytotoxicity of gelatin iron oxide nanoparticles

Cell viability after co-culture with gelatin iron oxide nanoparticles was evaluated with a cell counting kit (Nacalai Tesque Inc., Kyoto, Japan). The cells were seeded on each well of 96 multi-well cluster plate (Corning Inc., NY, USA)

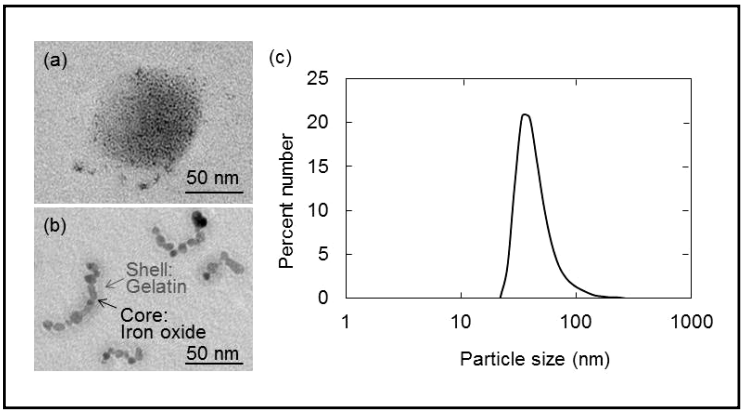

Fig.2 Transmission electron microscopy (TEM) images of gelatin iron oxide nanoparticles prepared by the micro-emulsion (a) and co-precipitation methods (b). (c)Hydrodynamic size distribution of gelatin iron oxide nanoparticles prepared by the micro-emulsion method.

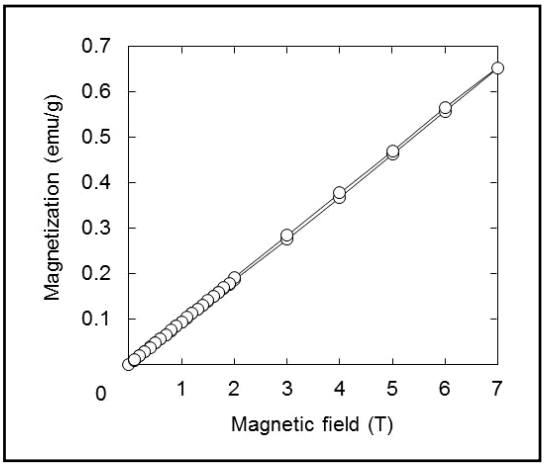

Fig.3 Magnetization curve of gelatin iron oxide nanoparticles prepared by the micro-emulsion method.

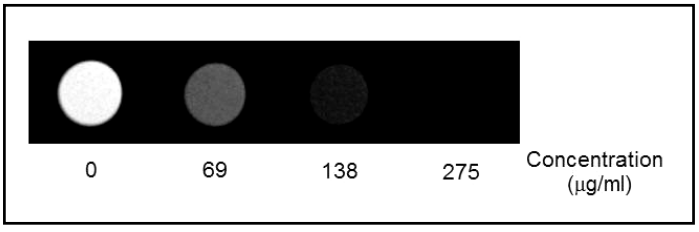

Fig.4 T_2-weighted MRI images of gelatin iron oxide nanoparticles prepared by the micro-emulsion method at different concentrations.

at a density of 5 × 10^3 cells/well and cultured in 100 μl of medium. After 24 hr of incubation, the medium was exchanged by 100 μl of fresh medium containing gelatin iron oxide nanoparticles at concentrations of 10, 50, 100, 150, and 200 μg/ml, followed by 24 hr of incubation. Then, the cells were washed with PBS 3 times, and 100 μl of fresh medium was added. Next, 10 μl of 2-(2-methoxy-4-nitrophenyl)-3-(4-nitrophenyl)-5-(2,4-disulfophenyl)-2H -tetrazolium (WST-8) solution was added and the cells were incubated for further 4 hr. The absorbance of solution was measured at 450 nm on the VERSAmax microplate reader. The percentage of cell viability was expressed as 100 % for control cells cultured without nanoparticles.

Results

1)Characterization of gelatin iron oxide nanoparticles

Figure 1 shows the schematic representation of gelatin iron oxide nanoparticles prepared by the micro-emulsion method, and gelatin iron oxide nanoparticles prepared by the co-precipitation method. Figure 2 shows the TEM images of gelatin iron oxide nanoparticles prepared by the modified micro-emulsion and the conventional co-precipitation methods, and the hydrodynamic size distribution of gelatin iron oxide nanoparticles prepared by the micro-emulsion method. For the nanoparticles prepared by the micro-emulsion method, ultra-small iron oxide nanoparticles were homogeneously dispersed in the gelatin iron oxide composite. In contrast, the nanoparticles prepared by the co-precipitation method showed a structure of iron oxide core and gelatin shell. The average hydrodynamic size and zeta-potential of gelatin iron oxide nanoparticles prepared by the micro-emulsion method were 87 nm and -9.2 mV, respectively.

Figure 3 shows the magnetization curve of gelatin iron oxide nanoparticles prepared by the micro-emulsion method. The gelatin iron oxide nanoparticles exhibited no remanence and zero coercivity, which indicate the super-paramagnetic property of nanoparticles.

2)Magnetic resonance imaging (MRI) of gelatin iron oxide nanoparticles

Figure 4 shows the T_2-weighted MR images of gelatin

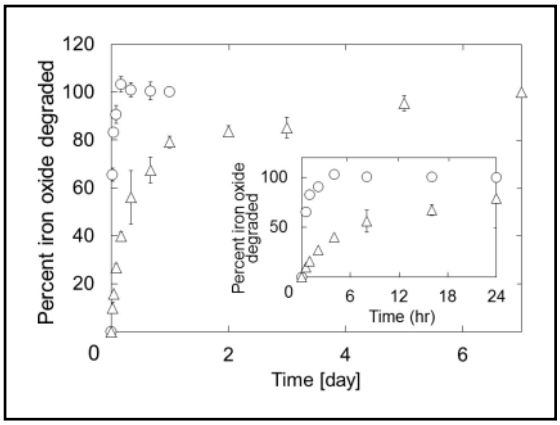

Fig.5 Time profiles of gelatin iron oxide nanoparticles degradation in 20 mM citric acid buffer at pH 4.5

The nanoparticles were prepared by the micro-emulsion (○) and co-precipitation methods (△).

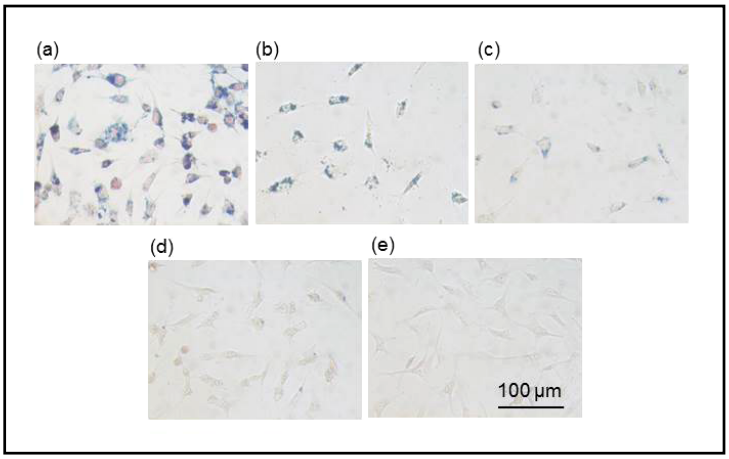

Fig.6 Prussian blue staining of gelatin iron oxide nanoparticles prepared by the micro-emulsion method in human mesenchymal stem cells

The cells were co-cultured with the nanoparticles for 24 hr (a), and after washing nanoparticles, the incubation was continued further for 1 (b), 2 (c), 4 (d), and 6 days (e).

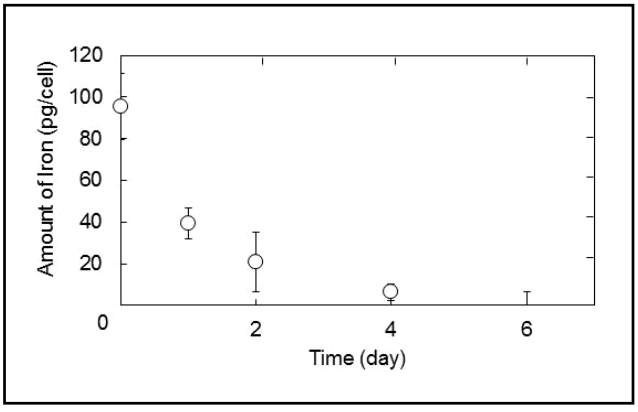

Fig.7 Time profiles of gelatin iron oxide nanoparticles degradation in human mesenchymal stem cells

The cells were co-cultured with the nanoparticles for 24 hr, and after washing nanoparticles, the incubation was continued further for 1, 2, 4, and 6 days.

iron oxide nanoparticles prepared by the micro-emulsion method at different concentrations dispersed in water. The images became stronger with an increase in the iron concentration. Transverse r_2 relaxivity was estimated to be 8.7 $(mmol/L)^{-1} \cdot s^{-1}$.

3) *In vitro* degradation test of gelatin iron oxide nano-particles

Figure 5 shows the time profiles of gelatin iron oxide nanoparticles degradation in the citric acid buffer. The degradation time of the gelatin iron oxide nanoparticles prepared with the modified micro-emulsion and the conventional co-precipitation methods was compared. The gelatin iron oxide nanoparticles prepared by the micro-emulsion method were degraded with time and disappeared within 4 hr. On the other hand, only 40 % of nanoparticles prepared by the co-precipitation method were degraded within 4 hr, and it took about 1 week for all of them to be degraded completely.

4) Cellular internalization of gelatin iron oxide nanoparticles and intracellular degradation

Figure 6 shows the prussian blue staining of gelatin iron oxide nanoparticles prepared by the micro-emulsion method in human mesenchymal stem cells. Figure 7 shows degradation time profile of gelatin iron oxide nanoparticles prepared by the micro-emulsion method in human mesenchymal stem cells. It is apparent that the gelatin iron oxide nanoparticles prepared by the micro-emulsion method were internalized into almost all of cells and localized in the cy-

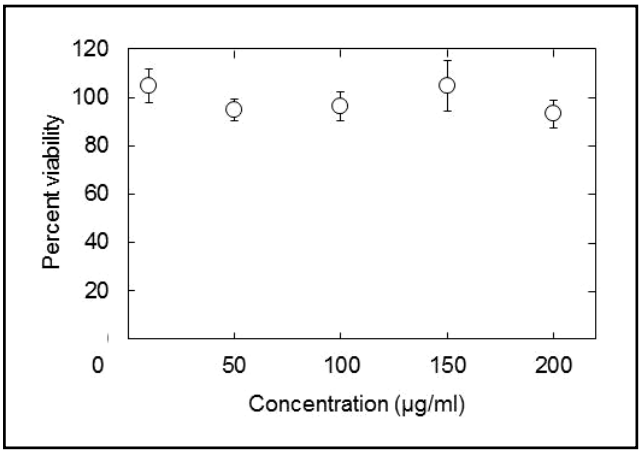

Fig.8 Viability of mesenchymal stem cells 24 hr after co-culture with gelatin iron oxide nanoparticles prepared by the micro-emulsion method at different concentrations.

toplasm at Day 0. The nanoparticles were degraded in the cells and the iron oxide disappeared with time. Degradation of gelatin iron oxide nanoparticles in cells was observed within 6 days. On the contrary, the nanoparticles prepared by the co-precipitation method were not internalized into the cells (data not shown).

5)Magnetic separation of mesenchymal stem cells

To evaluate whether or not the cells internalized by gelatin iron oxide nanoparticles magnetically respond, a neodymium magnet was exposed to the cells suspension. About 51% of cells were attracted by the magnet to separate.

6)Cytotoxicity of gelatin iron oxide nanoparticles

Figure 8 shows viability of mesenchymal stem cells 24 hr after co-culture with gelatin iron oxide nanoparticles prepared by the micro-emulsion method at different concentrations. Irrespective of the amount of nanoparticles cultured, the cell viability was equal to 100 %.

Discussion

Co-precipitation method is the most conventional method for synthesizing iron oxide nanoparticles. The particles are synthesized by co-precipitation of ferrous and ferric ions. For iron oxide nanoparticle synthesis, alkaline solution is added to an aqueous mixture of ferrous and ferric ions at a molar ratio of 1:2[27]. Co-precipitation of iron ions is often taken place in the presence of polymers to prevent the agglomeration of iron oxide. The resulted iron oxide nanoparticles have the structure of iron oxide core and polymer shell (Fig.1(b)). The core-shell gelatin iron oxide nanoparticles were prepared with the presence of gelatin in the conventional co-precipitation method.

On the contrary, modified micro-emulsion method was used to synthesize ultra-small iron oxide nanoparticles dispersed in the matrix of gelatin to improve the degradability of iron oxide. The preparation of gelatin nanoparticles and iron oxide nanoparticles by a micro-emulsion method has been reported separately[28, 29]. In this study, gelatin iron oxide nanoparticles were prepared by the combination of the two micro-emulsion methods (Fig.1(a)). Considering the preparation process, at the first step, ferric ions are interacted with the carboxyl groups of gelatin. After the addition of ferrous ions to the complex of ferric ions and gelatin chains, the nano-sized emulsions of the resulting solution were prepared to form nanoparticles of ferrous ions and the complex of ferric ions and gelatin. The nucleation and growth of iron oxide nanoparticles will take place in the nano-sized emulsions through co-precipitation of ferrous ions and ferric ions interacted with gelatin. In the conventional co-precipitation method, the simultaneous addition of ferric and ferrous ions results in the formation of larger size iron oxide nanoparticles. On the contrary in the micro-emulsion method, the existence of gelatin chains in the reaction area will prevent formation of the large particles during the growth process of iron oxide nanoparticles, and consequently the size of iron oxide nanoparticles become small.

Various types of iron oxide nanoparticles have been investigated for MRI contrast agents[2, 26, 28, 30, 31]. However, considering the biomedical applications of iron oxide nanoparticles, the nanoparticles should have a superparamagnetic property to avoid aggregation and give a large surface-to-volume ratio. It is reported that Fe_3O_4 nanopar-

ticles with the particle sizes of 7.5 and 13 nm are superparamagnetic, while the particles larger than 46 nm are ferromagnetic[30]. Gelatin iron oxide nanoparticles prepared by the micro-emulsion method exhibited a superparamagnetic property and MRI detectability (Fig.3 and 4). The transverse R_2 relaxivity of the nanoparticles was 8.7 $(mmol/L)^{-1} \cdot s^{-1}$. The R_2 relaxivity was lower than that of iron oxide nanoparticles with the particle sizes of 4.6 nm and 1.7 nm. The R_2 relaxivities of them were 34.8 and 15.01 $(mmol/L)^{-1} \cdot s^{-1}$, respectively[2, 31]. The MRI detectability of iron oxide nanoparticles strongly depends on their sizes[3]. This indicates that the iron oxides of gelatin iron oxide nanoparticles have an ultra-small particle size.

On the other hand, the R_1 relaxivity of the gelatine iron oxide nanoparticles was 0.03 $(mmol/L)^{-1} \cdot s^{-1}$. The R_1 relaxivity was lower than that of iron oxide nanoparticles with the particle sizes of 4.6 nm and 1.7 nm. The R_1 relaxivities of them were 16.5 and 4.46 $(mmol/L)^{-1} \cdot s^{-1}$, respectively. It has been suggested that iron oxide nanoparticles with the particle size of less than 4 nm could suppress the T_2 effect and possible to be the candidates for T_1 contrast agent[32]. However, when there are aggregations of the iron oxide nanoparticles, R_1 relaxivity tends to increase and R_2 relaxivity decreases[33]. Those suggest that the lower R_1 relaxivity compared to those nanoparticles with the particle sizes of 7.5 and 4.6 nm was caused by aggregation of the gelatin iron oxide nanoparticles during the MRI measurement.

The degradation of gelatin iron oxide nanoparticles prepared by the micro-emulsion method was much faster than that of nanoparticles prepared by the co-precipitation method. The faster degradation of gelatin iron oxide nanoparticles can be explained in terms of their unique structure and ultra-small particle size. Scotland et al. reported the degradation of Clariscan™ in citrate or acetate buffers at different pHs[17]. Clariscan™ was almost completely solubilized within 4-7 days with time in a citrate buffer at pH 4.5. Arbab et al. reported the degradation of ferumoxides complexed with poly-L-lysine in seven buffers containing different chelate agents at different pHs[18]. Ferumoxides are rapidly degraded with time in a citric acid buffer at pH 4.5 and disappeared within 7 days. Some researchers demonstrate the dissolution of hematite particles in the solution containing chelating agents[34, 35] and citric acid[36]. Chang et al. report that the surface complexation of the metal ions with chelating species weakens the lattice bonds between the ferric ion and oxygen, and consequently allows to release the entire complex into solution[34]. The findings suggest that chelating agents efficiently trap iron ions of iron oxide nanoparticles, and dissolves iron oxide nanoparticles. In this degradation study, crosslinked gelatin around iron oxide nanoparticles was not degraded in citric acid buffer, while iron oxides were dissolved into ferric and ferrous ions. It is known that gelatin is degraded by lysosomal proteases such as cathepsin B[37]. The degradability of gelatin is controlled by the degree of crosslinking[3]. Taken together, the degradability of gelatin iron oxide nanoparticles will be able to control by changing the condition of gelatin crosslinking.

Localization of gelatin iron oxide nanoparticles in the cytoplasm corresponds to the previous result[26], although they have a negative zeta potential. Cellular internalization of nanoparticles is greatly influenced by their shape, size, and surface functionality[38]. Some studies have indicated efficient cellular internalization of positively charged particles[26, 39]. On the other hand, there is the evidence of cellular uptake of negatively charged particles[40]. Even greater internalization of negatively charged particles has been reported[41].

Small molecules including amino acids, sugars, and ions, are transported into cells through the integral membrane protein pumps or channels, while other macromolecules are internalized through endocytosis[42]. The nanoparticles internalized were found in the phagolysosome of endosome-lysosome fusion[43, 44]. After cellular internalization, the gelatin iron oxide nanoparticles will be localized in phagolysosome, in which the degradation of iron oxide nanoparticles occurs at low pH[18]. Gelatin is degraded enzymatically in the phagolysosome. The gelatin iron oxide nanoparticles prepared by the micro-emulsion method disappeared in the cells fast compared with other research results. It has been reported that ferumoxides complexed with poly-L-lysine disappeared from rapidly dividing HeLa cells by 2.3 weeks and retained in mesenchymal stem cells at 44 days following the internalization[19]. It is highly conceivable that faster degradation of gelatin iron oxide nanoparticles is caused by their unique structure and ultra-small particle size as indicated by the *in vitro* degradation in the citric acid buffer solution. These results indicate that the biodegradable iron oxide nanoparticles which are potential for MRI contrast agent could be prepared by the micro-emulsion method in this study.

The magnetic separation of cells internalizing gelatin iron

oxide nanoparticles was achieved even though their small magnetization. As shown in figure 6, it is apparent that the gelatin iron oxide nanoparticles formed clusters after internalized into human mesenchymal stem cells. It has been known that iron oxide nanoparticles tend to form their clusters in phagolysosome after the cellular internalization[45], and the clusters of magnetic nanoparticles facilitates the magnetic separation[46].

Gelatin has been widely used for medical applications, which has proven the biocompatibility[46]. On the contrary, the biocompatibility of iron oxide nanoparticles is still in discussion[48-50]. In this study, the cell viability test demonstrates that mesenchymal stem cells were vivid after they internalized gelatin iron oxide nanoparticles.

Conclusions

Biodegradable iron oxide nanoparticles were successfully prepared with bioabsorbable gelatin by a micro-emulsion method with the slight modification. The gelatin iron oxide nanoparticles prepared by the micro-emulsion method showed the degradability in the low pH solution, in remarked contrast to those prepared by the conventional co-precipitation method. The gelatin iron oxide nanoparticles were internalized into bone marrow-derived mesenchymal stem cells and degraded intracellularly. The T_2-weighted signals of the gelatin iron oxide nanoparticles show their potential for magnetic resonance imaging.

Acknowledgements and Source of Funding

This work was supported by a Grant-in-Aid for JSPS Fellows. Magnetic property measurement was carried out using facilities of Research Center for Low Temperature and Materials Sciences, Kyoto University.

Conflict of interests

No conflicts of interest to be disclosed.

References

1) Arruebo M, Fernandez-Pacheco R, Ibarra MR, Santamaria J: Magnetic nanoparticles for drug delivery. Nanotoday. 2007; 2: 22-32.
2) Shen T, Weissleder R, Papisov M, Bogdanov A, Brady TJ: Monocrystalline iron oxide nanocompounds (MION): Physicochemical properties. Magn Reson Med. 1993; 29: 599-604.
3) Jun Y, Huh Y, Choi J, Lee J, Song H, Kim S, Yoon S, Kim K, Shin J, Suh J, Cheon J: Nanoscale Size Effect of Magnetic Nanocrystals and Their Utilization for Cancer Diagnosis via Magnetic Resonance Imaging. J Am Chem Soc. 2005; 127: 5732-5733.
4) Namiki Y, Namiki T, Yoshida H, Ishii Y, Tsubota A, Koido S, Nariai K, Mitsunaga M, Yanagisawa S, Kashiwagi H, Mabashi Y, Yumoto Y, Hoshina S, Fujise K, Tada N: A novel magnetic crystal.lipid nanostructure for magnetically guided in vivo gene delivery. Nature Nanotechnol. 2009; 4: 598-606.
5) Kami D, Takeda S, Itakura Y, Gojo S, Watanabe M, Toyoda M: Application of Magnetic Nanoparticles to Gene Delivery. Int J Mol Sci. 2011; 12: 3705-3722.
6) Yavuz CT, Mayo JT, Yu WW, Prakash A, Falkner JC, Yean S, Cong L, Shipley HJ, Kan A, Tomson M, Natelson D, Colvin VL: Low-Field Magnetic Separation of Monodisperse Fe_3O_4 Nanocrystals. Science. 2006; 314: 964-967.
7) Tomitaka A, Ueda K, Yamada T, Takemura Y: Heat dissipation and magnetic properties of surface-coated Fe_3O_4 nanoparticles for biomedical applications. J Magn Magn Mater. 2012; 324: 3437-3442.
8) Hofmann A, Thierbach S, Semisch A, Hartwig A, Taupitz M, Ruhl E, Graf C: Highly monodisperse water-dispersable iron oxide nanoparticles for biomedical applications. J Mater Chem. 2010; 20: 7842-7853.
9) Park J, Lee E, Hwang N, Kang M, Kim SC, Hwang Y, Park J, Noh H, Kim J, Park J, Hyeon T: One-Nanometer-Scale Size-Controlled Synthesis of Monodisperse Magnetic Iron Oxide Nanoparticles. Angew Chem. 2005; 117: 2932-2937.
10) Cole AJ, David AE, Wang J, Galban CJ, Yang VC: Magnetic brain tumor targeting and biodistribution of long-circulating PEG-modified, cross-linked starch-coated iron oxide nanoparticles. Biomaterial. 2011; 32: 6291-6301.
11) Chertok B, David AE, Yang VC: Polyethyleneimine-modified iron oxide nanoparticles for brain tumor drug delivery using magnetic targeting and intra-carotid administration. Biomaterial. 2010; 31: 6317-6324.
12) Park S, Kim HS, Kim WJ, Yoo HS: Pluronic@Fe_3O_4 nanoparticles with robust incorporation of doxorubicin by thermo-responsiveness. Int J Pharm. 2012; 424: 107-114.
13) Kayal S, Ramanujan RV: Doxorubicin loaded PVA coated iron oxide nanoparticles for targeted drug delivery. Mater Sci Eng C. 2010; 30: 484-490.

14) Maity D, Agrawal DC: Synthesis of iron oxide nanoparticles under oxidizing environment and their stabilization in aqueous and non-aqueous media. J Magn Magn Mater. 2007; 308: 46-55.
15) Zhao M, Kircher MF, Josephson L, Weissleder R: Differential Conjugation of Tat Peptide to Superparamagnetic Nanoparticles and Its Effect on Cellular Uptake. Bioconjugate Chem. 2002; 13: 840-844.
16) Xu H, Aguilar ZP, L. Yang L, Kuang M, Duan H, XiongY, Wei H, Wang A: Antibody conjugated magnetic iron oxide nanoparticles for cancer cell separation in fresh whole blood. Biomaterial. 2011; 32: 9758-9765.
17) Skotland T, Sontum PC, Oulie I: In vitro stability analyses as a model for metabolism of ferromagnetic particles (Clariscan™), a contrast agent for magnetic resonance imaging. J Pharma Biomed Anal. 2002; 28: 323-329.
18) Arbab AS, Wilson LB, Ashari P, Jordan EK, Lewis BK, Frank JA: A model of lysosomal metabolism of dextran coated superparamagnetic iron oxide (SPIO) nanoparticles: implications for cellular magnetic resonance imaging. NMR Biomed. 2005; 18: 383-389.
19) Arbab AS, Bashaw LA, Miller BR, Jordan EK, Lewis BK, Kalish H, Frank JA: Characterization of Biophysical and Metabolic Properties of Cells Labeled with Superparamagnetic Iron Oxide Nanoparticles and Transfection Agent for Cellular MR Imaging. Radiology. 2003; 229: 838-846.
20) Fukunaka Y, Iwanaga K, Morimoto K, Kakemi M, Tabata Y: Controlled release of plasmid DNA from cationized gelatin hydrogels based on hydrogel degradation. J Control Release. 2002; 80: 333-343.
21) Tabata Y, Ikada Y: Vascularization effect of basic fibroblast growth factor released from gelatin hydrogels with different biodegradabilities. Biomaterial. 1999; 20: 2169-2175.
22) Kohara H, Tabata Y: Enhancement of ectopic osteoid formation following the dual release of bone morphogenetic protein 2 and Wnt1 inducible signaling pathway protein 1 from gelatin sponges. Biomaterial. 2011; 32: 5726-5732.
23) Matsui M, Tabata Y: Enhanced angiogenesis by multiple release of platelet-rich plasma contents and basic fibroblast growth factor from gelatin hydrogels. Acta Biomaterialia. 2012; 8: 1792-1801.
24) Doi N, Jo J, Tabata Y: Preparation of Biodegradable Gelatin Nanospheres with a Narrow Size Distribution for Carrier of Cellular Internalization of Plasmid DNA. J Biomater Sci. 2012; 23: 991-1004.
25) Ishikawa H, Nakamura Y, Jo J, Tabata Y: Gelatin nanospheres incorporating siRNA for controlled intracellular release. Biomaterial. 2012; 33: 9097-9104.
26) Jo J, Aoki I, Tabata Y: Design of iron oxide nanoparticles with different sizes and surface charges for simple and efficient labeling of mesenchymal stem cells. J Control Release. 2010; 142: 465-473.
27) Gupta AK, Gupta M: Synthesis and surface engineering of iron oxide nanoparticles for biomedical applications. Biomaterial. 2005; 26: 3995-4021.
28) Allouche J, Boissiere M, Helary C, Livageab J: Biomimetic core.shell gelatine/silica nanoparticles: a new example of biopolymer-based nanocomposites. J Mater Chem. 2006; 16: 3120-3125.
29) Gupta AK, Wells S: Surface-Modified Superparamagnetic Nanoparticles for Drug Delivery: Preparation, Characterization, and Cytotoxicity Studies. IEEE Trans Nanobiosci. 2004; 3: 66-73.
30) Ma M, Wu Y, Zhou J, Sun Y, Zhang Y, Gu N: Size dependence of specific power absorption of Fe_3O_4 particles in AC magnetic field. J Magn Magn Mater. 2004; 268: 33-39.
31) Park JY, Daksha P, Lee GH, Woo S, Chang Y: Highly water-dispersible PEG surface modified ultra small superparamagnetic iron oxide nanoparticles useful for target-specific biomedical applications. Nanotechnology. 2008; 19: 365603.
32) Wan J, Jiang X, Li H, Chen K: Facile synthesis of zinc ferrite nanoparticles as non-lanthanide T1 MRI contrast agents. J Mater Chem. 2012; 22: 13500-13505.
33) Caravan P: Cardiovascular Magnetic Resonance Contrast Agents; Cardiovascular Magnetic Resonance. (eds. Manning WJ, Pennell DJ), Saunders/Elsevier, Philadelphia, PA; 2010, pp83.
34) Chang H, Matijevia E: Interactions of metal hydrous oxides with chelating agents: IV. Dissolution of hematite. J Colloid Interface Sci. 1983; 92: 479-488.
35) Taxiarchou M, Panias D, Douni I, Paspaliaris I, Kontopoulos A: Dissolution of hematite in acidic oxalate solutions. Hydrometallurgy. 1997; 44: 287-299.
36) Zhang Y, Kallay N, Matijevi E: Interactions of Metal Hydrous Oxides with Chelating Agents. 7. Hematite-Oxalic Acid and -Citric Acid Systems. Langmuir. 1985;

1: 201-206.
37) Ofner III CM, Pica K, Bowman BJ, Chen C: Growth inhibition, drug load, and degradation studies of gelatin/methotrexate conjugates. Int J Pharm. 2006; 308: 90-99.
38) Verma A, Stellacci F: Effect of Surface Properties on Nanoparticle. Cell Interactions. Small. 2010; 6: 12-21.
39) He C, Hu Y, Yin L, Tang C, Yin C: Effects of particle size and surface charge on cellular uptake and biodistribution of polymeric nanoparticles. Biomaterial. 2010; 31: 3657-3666.
40) Chung Y, Kim JC, Kim YH, Tae G, Lee S, Kim K, Kwon IC: The effect of surface functionalization of PLGA nanoparticles by heparin- or chitosan-conjugated Pluronic on tumor targeting. J Control Release. 2010; 143: 374-382.
41) Ryman-Rasmussen JP, Riviere JE, Monteiro-Riviere NA: Variables Influencing Interactions of Untargeted Quantum Dot Nanoparticles with Skin Cells and Identification of Biochemical Modulators. Nano Lett. 2007; 7: 1344-1348.
42) Conner SD, Schmid SL: Regulated portals of entry into the cell. Nature. 2003; 422: 37-44.
43) Xiao Y, Forry SP, Gao X, Holbrook RD, Telford WG, Tona A: Dynamics and mechanisms of quantum dot nanoparticle cellular uptake. J Nanobiotechnol. 2010; 8: 13.
44) Dash BC, Rethore G, Monaghan M, Fitzgerald K, Gallagher W, Pandit A: The influence of size and charge of chitosan/polyglutamic acid hollow spheres on cellular internalization, viability and blood compatibility. Biomaterial. 2010; 31: 8188-8197.
45) Daldrup-Link HE, Rudelius M, Oostendorp RAJ, Settles M, Piontek G, Metz S, Rosenbrock H, Keller U, Heinzmann U, Rummeny EJ, Schlegel J, Link TM: Targeting of Hematopoietic Progenitor Cells with MR Contrast Agents. Radiology. 2003; 228: 760-767.
46) Lai JJ, Hoffman JM, Ebara M, Hoffman AS, Estournes C, Wattiaux A, Stayton PS: Dual Magnetic-/Temperature-Responsive Nanoparticles for Microfluidic Separations and Assays. Langmuir. 2007; 23: 7385-7391.
47) Schrieber R, Gareis H: Medical Applications; Gelatine Handbook-Theory and Industrial Practice. Wiley-VCH, New York; 2007, pp255-259.
48) Gupta AK, Gupta M: Cytotoxicity suppression and cellular uptake enhancement of surface modified magnetic nanoparticles. Biomaterial. 2005; 26: 1565-1573.
49) Kim M, Jung J, Lee J, Na K, Park S, Hyun J: Amphiphilic comblike polymers enhance the colloidal stability of Fe3O4 nanoparticles. Colloids Surf B: Biointerface. 2010; 76: 236-240.
50) Kim DH, Kim KN, Kim KM, Lee YK: Targeting to carcinoma cells with chitosan- and starch-coated magnetic nanoparticles for magnetic hyperthermia. J Biomed Mater Res A. 2008; 88A: 1-11.